



# Minimal alteration of montmorillonite following long-term interaction with natural alkaline groundwater: Implications for geological disposal of radioactive waste



Antoni E. Milodowski <sup>a</sup>, Simon Norris <sup>b</sup>, W.Russell Alexander <sup>c,\*</sup>

<sup>a</sup> British Geological Survey (BGS), Keyworth NG12 5GG, UK

<sup>b</sup> Radioactive Waste Management Limited (RWM), Harwell OX11 ORH, UK

<sup>c</sup> Bedrock Geosciences, 5105 Auenstein, Switzerland

## ARTICLE INFO

### Article history:

Received 2 July 2015

Received in revised form

23 December 2015

Accepted 28 December 2015

Available online 31 December 2015

### Keywords:

Bentonite

Alkali leachates

Long-term reaction

Ion exchange

## ABSTRACT

Bentonite is one of the more safety-critical components of the engineered barrier system in the disposal concepts developed for many types of radioactive waste. Bentonite is utilised because of its favourable properties which include plasticity, swelling capacity, colloid filtration, low hydraulic conductivity, high retardation of key radionuclides and stability in geological environments of relevance to waste disposal. However, bentonite is unstable under the highly alkaline conditions induced by Ordinary Portland Cement (OPC: initial porewater pH > 13) and this has driven interest in using low alkali cements (initial porewater pH 9–11) as an alternative to OPC. To build a robust safety case for a repository for radioactive wastes, it is important to have supporting natural analogue data to confirm understanding of the likely long-term performance of bentonite in these lower alkali conditions. In Cyprus, the presence of natural bentonite in association with natural alkaline groundwater permits the zones of potential bentonite/alkaline water reaction to be studied as an analogy of the potential reaction between low alkali cement leachates and the bentonite buffer in the repository. Here, the results indicate that a cation diffusion front has moved some metres into the bentonite whereas the bentonite reaction front is restricted to a few millimetres into the clay. This reaction front shows minimal reaction of the bentonite (volumetrically, less than 1% of the bentonite), with production of a palygorskite secondary phase following reaction of the primary smectites over time periods of 10<sup>5</sup>–10<sup>6</sup> years.

© 2015 Elsevier Ltd. All rights reserved.

## 1. Introduction

Bentonite makes an important contribution to the performance of the engineered barrier system (EBS) for the disposal concepts developed for many types of radioactive waste (see Alexander and McKinley, 2007; for details). The choice of bentonite results from its favourable properties (plasticity, swelling capacity, colloid filtration, low hydraulic conductivity, high retardation of key radionuclides) for isolation and containment of the waste and its stability in relevant geological environments. However, bentonite – especially the swelling clay component (smectite) that contributes to its essential barrier functions – is unstable under high pH conditions. This led to some proposed repository designs that exclude use of

concrete from any sensitive areas containing bentonite. This is because cementitious leachates from OPC (Ordinary Portland Cement) will have an initial pH of greater than 13 (cf. Haworth et al., 1987). This option was considered acceptable during early, generic studies but, as projects move closer to implementation, it has been increasingly recognised that constructing extensive facilities underground without using concrete will be problematic (cf. Alexander and Neall, 2007; Alexander and McKinley, 2007).

Recently, therefore, there have been extensive efforts to better understand the interactions of alkaline fluids with bentonite (e.g. Savage et al., 2010a; Soler et al., 2011; Sidborn et al., 2015), coupled with studies aimed at reducing the potential risk by development (cf. NDA, 2010) and testing (e.g. Vuorinen et al., 2005; Ahokas et al., 2006; Savage and Benbow, 2007) of low alkali cement formulations which typically have leachates with a pH of 9–11. Attempts to examine the potential reaction of bentonite experimentally at these lower pH values have been complicated by the inherently slow

\* Corresponding author.

E-mail addresses: [aem@bgs.ac.uk](mailto:aem@bgs.ac.uk) (A.E. Milodowski), [simon.norris@nda.gov.uk](mailto:simon.norris@nda.gov.uk) (S. Norris), [russell@bedrock-geosciences.com](mailto:russell@bedrock-geosciences.com) (W.Russell Alexander).

kinetics of such reactions (e.g. Heikola et al., 2013). Clearly, this is an area where studying natural systems could play a valuable role – bridging the disparity in realism in temporal and spatial scales between laboratory studies and the systems represented in repository performance assessment (see discussion in Alexander et al., 1998, 2014, 2015; Miller et al., 2000). Indeed, in this case, the particularly slow kinetics of bentonite reaction in low alkali cement porewaters suggests natural system studies<sup>1</sup> would appear to be the only viable method of assessing bentonite reaction within a timescale which would allow input to current repository safety cases.

In this study, the Mediterranean island of Cyprus was the focus primarily due to the known widespread occurrence of both alkaline groundwaters (resulting from serpentinisation of the Troodos ophiolite; e.g. Neal and Shand, 2002) and extensive bentonite deposits (e.g. Bear, 1960) which constitute the base of the sedimentary carapace overlying the igneous sequences of the ophiolite. The details of the production of the alkaline groundwaters is discussed in Alexander et al. (2012), here it is sufficient to note that the chemistry of the natural groundwaters is similar enough to the leachates of low alkali cements to make this a viable natural analogue of the repository system (see discussion in Alexander et al., 2008, 2012). Although the natural bentonites are not identical to the processed bentonites<sup>2</sup> utilized in a repository, the differences in the relevant parameters are small enough to have little impact on the outcome of the study.

Based on previous work on the Zambales ophiolite in Luzon, Philippines (e.g. Alexander et al., 2008; Fujita et al., 2010), and on the Troodos ophiolite, Cyprus (e.g. Boronina et al., 2005; Alexander and Milodowski, 2011; Alexander et al., 2012), it appears that the alkali groundwaters generally interact with the base of the bentonite as they issue from underlying pillow lavas at the top of the ophiolite igneous sequence (Fig. 1). As the bentonite usually acts as an aquiclude, neutral surficial groundwaters generally lie above the bentonite.

## 2. Site description

Sampling was carried out around the abandoned village of Parsata, ENE of the town of Limassol (Fig. 2). The village sits on a plateau above the Vasilikos valley, which drains the Limassol Forest. The area offered the ideal combination of appropriate alkaline groundwaters in contact with bentonite and preliminary analysis of rock samples had shown abundant smectite and evidence of both current and formerly active alkaline groundwater flow systems. The bentonites are from the Turonian (90.4 Ma) Peripedhi Formation and are distributed over the palaeo-depressions in the Upper Pillow Lavas (UPL) as lenses of various thickness.

The UPL were deeply weathered in the submarine environment before the bentonites were laid down, but have also been extensively faulted since. In addition to this large scale earth movement, significant areas of the Vasilikos valley have suffered bentonite

debris flow and these generally raft bentonites and chalks of the overlying Kannaviou and Lower Lefkara Formations downslope over the Peripedhi Formation (see discussion in Alexander et al., 2012). As such, great care was taken to ensure that the sampling sites are not in allochthonous material.

## 3. Methods

Full details of the field campaign are presented in Alexander and Milodowski (2014). Briefly, over two field seasons at the Parsata site, a geomorphological analysis was carried out and ground penetrating radar (Malå Geoscience, Sweden) and resistivity studies (using a Schlumberger array) were conducted, all tied to a new local topographic grid produced with a RTK GPS (Trimble R6) system. Based on the data produced, four shallow (maximum depth 43 m) boreholes were air-drilled and five (2–3 m deep) trenches excavated in a 500 m<sup>2</sup> area around N 34° 49.500', E 033° 15.850', some 150 m to the south of Parsata village (Fig. 2). The thickness of the bentonitic Peripedhi Formation encountered in the boreholes and trenches varied considerably across the area, reflecting infilling of the highly irregular surface of the underlying UPL substrate. This is further complicated by local land-slides and gravitational mass movement associated with the steep topography of the area. The geological sequences for Trench 1 and Trench 4, on which this study focussed, are summarised in Fig. 3. Trench 5 was excavated near the deepest borehole in the bentonite so as to provide an example of unreacted material well above the bentonite-UPL contact.

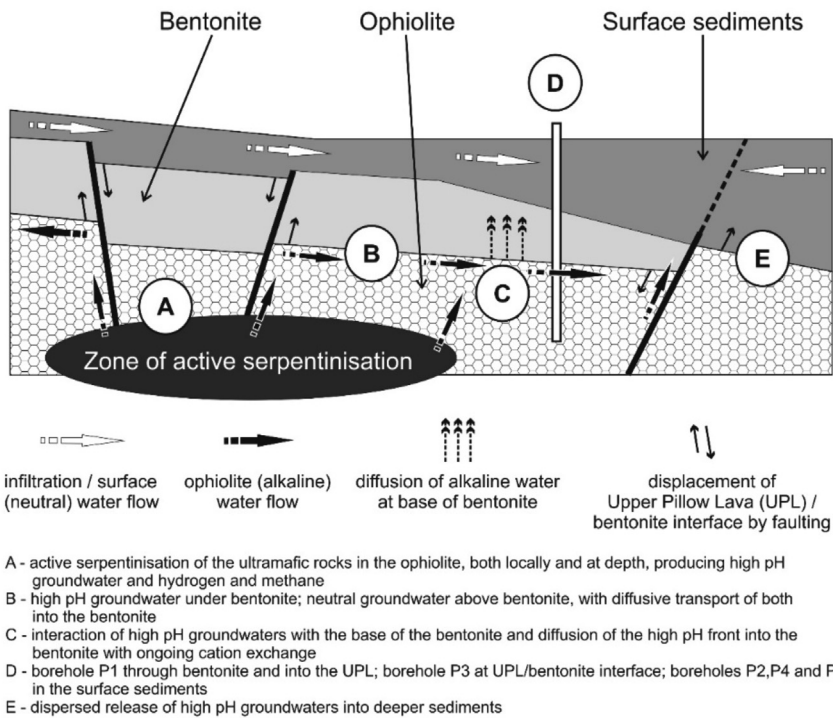
Small (10–100 g) solid phase samples were hand-picked from cores, drilling chips recovered from the boreholes and from the trench walls and floors, sealed in plastic film, wrapped in aluminium and then placed in airtight plastic containers for transport to the analytical laboratories. Large (500–2000 g) grab samples were also collected and an attempt was made to keep the individual samples as intact as possible by wrapping them in heavy-duty plastic and duct tape immediately upon sampling. In addition, large 50 × 100 mm aluminium soil-sampling (Kubiena) tins were used to collect undisturbed intact samples where possible.

Small solid phase samples were analysed by the British Geological Survey (BGS, UK) for particle-size distribution, whole-rock and clay mineralogy by X-ray diffraction (XRD) analysis (clay minerals quantified by Newmod-modelling: Reynolds and Reynolds, 1996), detailed petrography by optical petrographic microscopy, environmental scanning electron microscopy (ESEM), and energy-dispersive X-ray microanalysis (EDXA), major and trace element geochemistry by X-ray fluorescence spectroscopy (XRFS), cation exchange capacity (CEC) and exchangeable cations analysis. Large grab samples were analysed by Geoinvest (Cyprus) for natural moisture content, unconfined/uniaxial compressive strength tests, Atterberg Limits (liquid limits, plastic limits and plasticity index), swelling pressure and undrained triaxial tests.

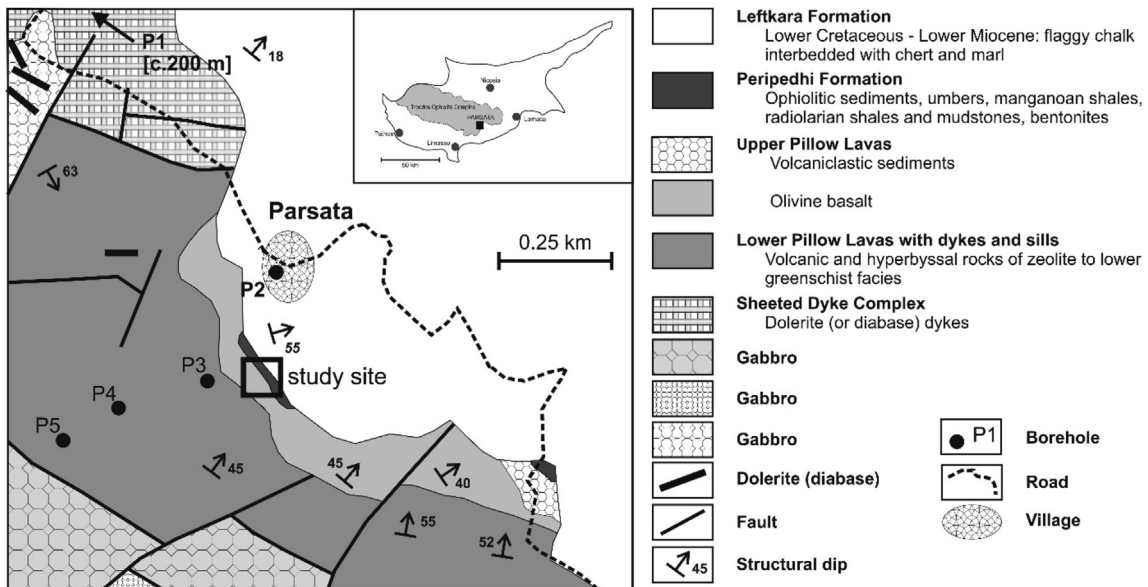
No groundwater was encountered in the site boreholes as these were completely within the exposed, unsaturated bentonite (i.e. no Lefkara Formation overburden, a local aquifer) and did not penetrate the underlying weathered UPL (which also constitutes an aquifer locally; A. Siathas, *pers comm.*, 2011). The bases of Trenches 1 and 4 did penetrate the UPL and these were noticeably moist upon excavation, although the pH of the moisture could not be ascertained due to the low volumes encountered. Groundwater samples were collected from five irrigation boreholes (P1 to P5, Fig. 2) drilled within 0.1–1 km of the site, with the aim of collecting waters typical of the geological formations present in the area. Licensed groundwater extraction borehole P1 draws groundwater from within the UPL sequence (underlying the Peripedhi bentonite), but boreholes P2 to P5 are unlicensed, so there is some

<sup>1</sup> The study of natural (predominantly geological) systems has been termed natural analogue research within the radioactive waste disposal community and the term "natural analogue" (NA) has developed a particular meaning associated with providing supporting arguments for a repository safety case (see Alexander et al., 2015 for details).

<sup>2</sup> The natural bentonite is usually processed (i.e. beneficiated) to improve the smectite content of the material. It is also usually chemically treated to enhance its cation exchange, swelling or other physico-chemical properties (e.g. conversion or "activation" of natural calcium montmorillonite to sodium montmorillonite by treatment with sodium carbonate). As such, the physical and chemical properties of processed bentonite may differ somewhat from that of the natural rock and this limitation must be borne in mind when considering the results.



**Fig. 1.** Conceptual model of groundwater flow in the Troodos ophiolite. The ophiolite-derived, natural alkali (high pH) groundwaters are in contact with the base of the Peripedhi bentonite while surficial (neutral pH) groundwaters flow across the top.

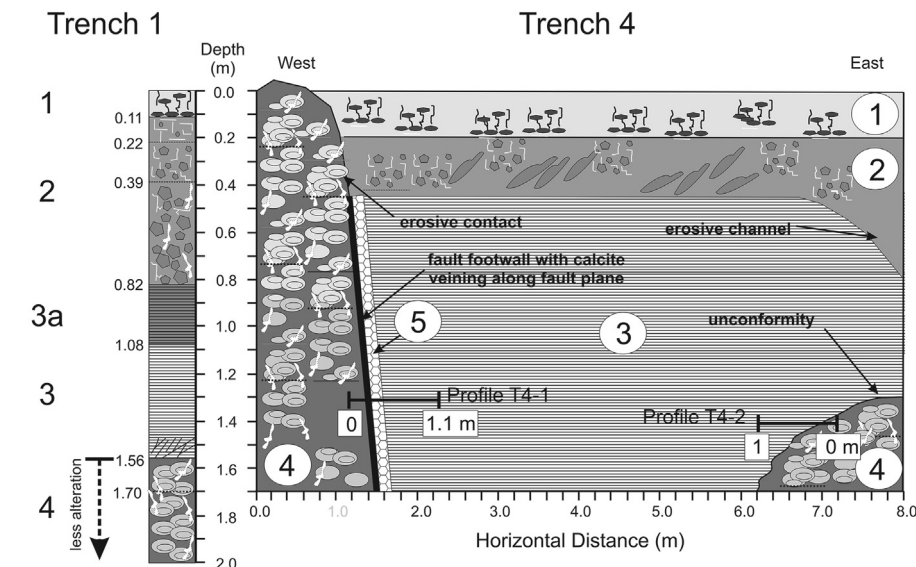


**Fig. 2.** Location map and bedrock geology of the Parsata area showing the location of study site (Alexander and Milodowski, 2015, after Gass et al., 1994). The geographical position of the irrigation boreholes used for groundwater sampling have been added for orientation purposes: see Table 1 for information on sampled horizons.

ambiguity as to the groundwater sources being sampled. From borehole depths and site characteristics, P2 is lying within the Leftkara Formation (overlying the Peripedhi bentonite) and P4 and P5 appear to be within rafted allochthonous Leftkara Formation material (not shown in Fig. 2). P3 is deeper than P4 and P5 and could reach as deep as the UPL, but it is unclear onsite.

Groundwater Eh, pH and temperature were recorded in the field and samples preserved employing a BGS standard methodology (see Kunimaru et al., 2011; Alexander and Milodowski, 2014 for

details). Samples were analysed for a suite of major and trace elements and stable isotopes in the Analytical Geochemistry Laboratories of BGS using a combination of inductively coupled plasma-atomic emission spectrometry (ICP-AES) for major cations (Ca, Mg, Na and K), inductively coupled plasma-mass spectrometry (ICP-MS) for the minor and trace cations, ion chromatography (IC) for anions, total organic carbon (TOC) by TOC analyser and colorimetry for reduced sulphur. Natural decay series nuclides were determined at SUERC (Scottish Universities Environmental

**Lithological summary:****1. Tilled "Terra Rossa" soil**

Up to 0.25 m of dark red-brown to chocolate-brown, highly fissured stony soil, with abundant chert and weathered chalky limestone and occasional basalt clasts up to 20 mm. Abundant roots.

**2. Debris flow deposit**

0.25 to c. 0.8 m of dark brown, compact, highly fissured soil with abundant chert and chalky limestone clasts up to 40 mm. The clasts are platy and blocky and aligned with a weakly imbricate structure indicating movement down-slope to the west. The deposit thickens in the eastern end of the trench, where it fills a channel-like feature eroded into the underlying laminated bentonite. Fissured with discontinuous fissures coated with thin (<1 mm) white, powdery  $\text{CaCO}_3$  and diffuse patches of white powdery  $\text{CaCO}_3$ .

**3. Laminated bentonite**

Hard, compact, fractured, finely-laminated mudstone. Buff-to chocolate-brown clay with very thin red-brown ferruginous partings and black manganese oxide-coated bedding partings. Dips 43° to N043°. The upper 0.26 m in Trench 1 is developed as a discrete manganese oxide-rich and goethite-free horizon, comprising finely-laminated mudstone with abundant very thin partings of black to metallic-grey manganese oxide, and small (1–2 mm) "nodules" and "dendrites" of manganese oxide along bedding planes (3a).

**4. Basaltic pillow lava**

Highly altered with argillised spheroidal (onion-skin) alteration rinds around relic "corestones" of black unaltered basalt. Green "soapy" altered clay matrix between basalt pillows. White, powdery secondary  $\text{CaCO}_3$  mineralisation forms coatings around the basalt pillows and fills subvertical, irregular fissures in the altered basalt.

**5. Sheared bentonite**

Brittle and highly sheared bentonite with fine, close-spaced fractures orientated parallel to the fault plane contact with the pillow lava at the western end of the trench. Fracture surfaces are polished and slicksided, and coated with white, powdery secondary  $\text{CaCO}_3$ , particularly in the lower part of the trench (<1 m depth).

**Fig. 3.** Schematic summary of the lithological sequence and descriptions of Trench 1 (vertical sequence) and Trench 4 (horizontal wall section showing sampling transects). The laminated bentonite (3) is from the Peripedi Formation and the debris flow deposits (2) appear to be from the upslope Leftkara Formation deposits.

Research Centre, UK). Full analytical methods, including analytical uncertainties, are described in detail in Alexander and Milodowski (2014).

## 4. Results

### 4.1. Hydrochemistry

The major element chemistry of the groundwaters in the Parsata area vary (see Table 1) from the ophiolite-sourced alkaline  $\text{Ca}-\text{Na}-\text{OH}-\text{SO}_4-\text{Cl}$ -type groundwater encountered in borehole

P1 to neutral  $\text{Ca}-\text{Mg}-\text{Na}(\text{K})-\text{HCO}_3-\text{Cl}-\text{SO}_4$  type groundwater of boreholes P2, P4 and P5. P2 has a notably high nitrate concentration ( $\text{NO}_3^- = 359 \text{ mgL}^{-1}$ ), probably reflecting contribution from the livestock farm in the immediate vicinity.

The P3 borehole is about 125 m southwest of the study site and this water is moderately alkaline ( $\text{pH}$  nearly 9) and Mg and nitrate are low, only slightly higher than that of the alkaline groundwater P1. Ca is very low compared to any of the other waters and this may result from interaction with the bentonite. Certainly cation exchange analysis of reacted bentonite in Trench 4 shows that significant Ca exchange occurs where the bentonite close to the

**Table 1**

Major element concentrations ( $\text{mgL}^{-1}$ ) for groundwater from boreholes P1 to P5 at Parsata. Trace element data are presented in Table S1, Supplementary Data.

Borehole	Formation sampled	Eh mV	Field pH	Lab pH	$\text{Ca}^{2+}$	$\text{Mg}^{2+}$	$\text{Na}^+$	$\text{K}^+$	$\text{CO}_3^{2-}$	$\text{HCO}_3^-$	$\text{OH}^-$	$\text{Cl}^-$	$\text{SO}_4^{2-}$	$\text{NO}_3^-$
P1	UPL	-210	11.05	10.9	49.8	0.04	110	1.1	6.04	<5.00	17.5	86.0	156	0.101
P2	Leftkara	+7.9	7.48	7.75	172	25.1	175	48.5	no data	203	no data	324	88.6	359
P3	possibly UPL	-0	8.92	8.67	4.8	0.40	297	0.8	19.5	217	no data	130	245	0.895
P4	allochthonous Leftkara	-38	7.28	8.10	78.4	71.3	277	2.2	no data	692	no data	170	296	12.6
P5	allochthonous Leftkara	-31	7.38	7.63	79.6	48.9	206	3.3	no data	673	no data	108	101	24.8

contact with the underlying UPL has reacted with alkali groundwater (Section 4.5).

The minor and trace element data for the five groundwaters (Table S1 in the Supplementary Data) generally reflect the above noted major element data pattern. The Li/Cl and B/Cl ratios of the Parsata groundwaters are of particular interest as Davies and Elderfield (2004) noted that Li is preferentially leached during early stages of high temperature serpentinisation of ocean crust and that the Li/Cl and B/Cl ratios provide a useful guide to the fluid/rock mass ratios. Alexander and Milodowski (2011) and Alexander et al. (2012) reported B/Cl ratios of between and  $4.2\text{--}4.4 \times 10^{-3}$  for alkali springs on the Troodos Massif, somewhat greater than that of seawater ( $3.3 \times 10^{-3}$ ; Kreitler and Bledsoe, 1993). P1, in comparison, has a B/Cl ratio of  $9.7\text{--}10.8 \times 10^{-3}$ , indicating B enrichment.

However, B is anomalously high ( $2976 \mu\text{g L}^{-1}$ ) in groundwater P3 compared to the other groundwaters and the B/Cl ratio is the highest observed at  $22.9 \times 10^{-3}$  (cf. P2, P4 and P5 at  $1.1\text{--}2.6 \times 10^{-3}$ ). Petrographic evidence (Section 4.4) shows that, in addition to a very high content of smectite, the Parsata bentonites also have a large amount of amorphous or biogenic silica. Boron is strongly sorbed from seawater onto clay minerals and biogenic silica sediments in the marine environment and then is re-released during diagenesis (e.g. Truscott and Shaw, 1984; Ishikawa and Nakamura, 1993), or liberated from the clays by rock–water interaction (Alexander, 1985). The high concentration of B (and the much higher B/Cl ratio) found in the P3 groundwater could derive from interaction of a P1-type alkaline groundwater with the bentonite.

Limited stable isotope, strontium isotope and natural decay series data (Table 2) suggest that the groundwater from all five Parsata boreholes have a common source. Comparison of the stable isotope data with those from the Troodos ophiolite (Alexander et al., 2012) and from the much larger dataset for the nearby Kouris valley catchment (Boronina, 2003) imply that the infiltration area is some 200–300 m higher than Parsata, presumably on the ridge about 1.5 km NE of the village.

The groundwater  $^{87}\text{Sr}/^{86}\text{Sr}$  ratios appear to show a similar trend to that noted above from P1 (least radiogenic), through P3 (intermediate) to P4, P5 and P2 (most radiogenic). The intermediate  $^{87}\text{Sr}/^{86}\text{Sr}$  ratio for P3 could be accounted for by mixing of an alkaline groundwater from the ophiolite basement (P1-type) with groundwater from the overlying calcareous sedimentary strata. However, as the P3  $^{87}\text{Sr}/^{86}\text{Sr}$  isotope ratio of  $0.707253 (\pm 6)$  is very close to that of the fresh UPL ( $0.707302 \pm 6$ ; section 4.5), this suggests that P3 is an ophiolite alkali groundwater that has undergone some reaction with bentonite, but not yet sufficiently to lose the original  $^{87}\text{Sr}/^{86}\text{Sr}$  signature.

The  $^{234}\text{U}/^{238}\text{U}$  activity ratios for all four groundwater samples measured are indistinguishable within the analytical errors. The data are therefore consistent with a single source of uranium, but with the expected (cf. Linklater et al., 1996) significantly lower solubility of uranium in the alkaline groundwater (P1) than in P2 and P4 with the P3 activity concentration, once again, lying

between these two end members.

#### 4.2. Bentonite physico-chemical properties

In most national radioactive waste disposal programmes, there are guidelines (e.g. Ahonen et al., 2008) for the physico-chemical properties of the processed bentonites which will be utilised as buffer and backfill in the repository. Therefore, to define the degree of similarity between the natural bentonites at Parsata and the repository processed bentonites, a selection of samples was taken for definition of a range of bentonite material properties and these are shown in Table 3 (the full dataset is listed in Table S2 of the Supplementary Data).

It can be seen from Table 3 that, despite the non-processed nature of the natural bentonite, most of the parameters fall within or are close to example guideline values for the processed bentonite. Only in swelling pressure, a reflection of the low smectite content, is there a significant deviation, with the natural bentonite being much lower. Indeed, as noted in Alexander and Milodowski (2014), the swelling pressures (Table S2) are more comparable with the processed bentonite/crushed rock or sand mixtures foreseen in some repository designs (e.g. McKinley et al., 2007).

#### 4.3. Mineralogy

The results of the bulk mineralogical analyses are summarised in Fig. 4a (and full details are provided in Tables S3 and S4 of the Supplementary Data). Initial investigations, reported previously by Alexander and Milodowski (2011) and Alexander et al. (2012, 2013), were based on transects sampled vertically through the bentonite from the four shallow boreholes and Trench 1. However, no systematic variation in mineralogy could be discerned with depth that might reflect interaction with alkaline groundwater penetrating the bentonite from the underlying basaltic pillow lavas (Figs. 1 and 3), and any variations could not readily be differentiated from primary stratigraphic-sedimentary depositional controls. Subsequently, Trench 4 facilitated sampling along bedding-parallel horizontal transects within two discrete bedding horizons, from the contact with the UPL into the overlying bentonite. The majority of samples taken along both transects (Fig. 3) are predominantly composed of clay-grade material (Fig. 4a). The bentonite along these transects shows little lateral variation in grain size, indicating that there is no obvious lateral primary lithological variation and that any mineralogical variations most likely reflect reaction with groundwater from the underlying UPL aquifer.

The bentonite and altered UPL samples are predominantly composed of smectite (24–50%, mean 31%), quartz (1–13%, mean 11%), zeolites (0–18%, mean 10%) and amorphous material (18–32%, mean 25%). No systematic variation in smectite or amorphous material is apparent along either transect within the bentonite (Fig. 4b). SEM analysis indicates that much of amorphous material in the bentonite is predominantly biogenic silica (from

**Table 2**

Stable isotope,  $^{87}\text{Sr}/^{86}\text{Sr}$  isotope ratio and natural decay series data for groundwater from boreholes P1 to P5 at Parsata (quoted uncertainties are  $2\sigma$ ).

Sample id	$\delta^{18}\text{O}$	$\delta^2\text{H}$	$^{87}\text{Sr}/^{86}\text{Sr}$	$^{238}\text{U}$ (mBq $\text{L}^{-1}$ )	$^{234}\text{U}$ (mBq $\text{L}^{-1}$ )	$^{234}\text{U}/^{238}\text{U}$
	‰VSMOW	‰VSMOW				
P1	-4.64	-22.6	$0.706825 \pm 0.000006$	$0.41 \pm 0.08$	$0.62 \pm 0.10$	$1.5 \pm 0.4$
P2	-5.28	-26.7	$0.708020 \pm 0.000008$	$9.3 \pm 0.3$	$11.9 \pm 0.3$	$1.28 \pm 0.05$
P3	-4.61	-24.4	$0.707253 \pm 0.000006$	$1.8 \pm 0.4$	$3.3 \pm 0.6$	$1.8 \pm 0.5$
P4	-4.25	-21.2	$0.707743 \pm 0.000006$	$45.4 \pm 0.7$	$60.0 \pm 0.9$	$1.32 \pm 0.03$
P5	-4.25	-21.6	$0.707829 \pm 0.000007$	no data	no data	no data

**Table 3**

Values for some selected physical parameters of the Parsata natural bentonites compared with example guidelines (Ahonen et al., 2008) for repository processed bentonites.

Parameter	Dry density kg m <sup>-3</sup>	Gravimetric water content % <sup>a</sup>	Smectite content %	Liquid limit %	CEC meq 100g <sup>-1</sup>	Swelling pressure MPa
Guidelines	1655–1890 <sup>b</sup>	<13	>75	>80	>60	1–10
Trench 4	1340–1430	18–25	26–50	74–89	47–59	0.09–0.14
Trench 5	1340–1390	17–23	24–28	106–131	34–43	0.12–0.17

<sup>a</sup> relative to the sample dry weight.

<sup>b</sup> Depending on the specific design concept under consideration.

siliceous tests). Other minor components include calcic plagioclase feldspar, undifferentiated ‘mica’ (illite and detrital micas), palygorskite and calcite ± K-feldspar, cristobalite, tridymite, pyroxene, manganite, goethite, pyrolusite, chlorite and amphibole, and these also show little variation within the bentonite.

Calcite contents are typically ~2% but increase markedly to ~10% in the mineralised and sheared bentonite faultrock at the contact between the altered UPL and bentonite in transect 4-2 (Fig. 3). XRD analysis also indicates that the calcite present in the bentonite in transect 4-1 is Mg-rich compared to that present in the altered UPL whereas, in transect 4-2, the calcite is a mixture of Mg-rich and Mg-poor calcite. Clinoptilolite-heulandite was found in all bentonite samples and traces of stilbite (<0.5%) were also identified in one sample from transect 4-2 and one sample in Trench 5. Zeolite minerals are more abundant in transect 4-2 and Trench 5 than in Trench 1, and probably reflect primary stratigraphic-sedimentary differences between the horizons in the bentonite.

Quantitative <2 μm fraction XRD analyses (Table S5 of the Supplementary Data) indicate that the clay mineral assemblages are predominantly composed of smectite with minor amounts of palygorskite and illite and traces of chlorite. In all cases, the separated <2 μm fractions also contain a variety of non-clay minerals including quartz, albite, zeolite and possibly calcite. The smectite  $d_{000}$  spacings in the bentonite (mean 1.5067 ± 0.0020) are close to ideal montmorillonite. Little systematic variation in smectite (77–91%), illite (9–20%) or chlorite (0–4%) content with distance from the faulted contact with the UPL is visible in transect 4-1 (Fig. 4b). A slight decrease in smectite, associated with a slight increase in illite, was observed with increasing distance from the UPL contact in transect 4-2 (Fig. 4c). However, the scale of the variation in mineralogy is broadly similar to that seen in Trench 5 (Table S5).

#### 4.4. Petrology

The petrography of the Peripedhi bentonite is described in detail in Alexander et al. (2012) and Alexander and Milodowski (2015) and it consists of finely laminated chocolate-brown to orange-brown mudstones and silty mudstones. They are dominated by a matrix of detrital smectitic and illitic clay minerals, with minor matrix-supported, silt-grade quartz, feldspar (mainly plagioclase), micas (mostly biotite with lesser muscovite), chlorite and apatite. The lamination is defined by colour, silt content, and the alignment of elongate detrital grains. Some syn-depositional deformation of the lamination is apparent, possibly from dewatering and/or localised slumping. The bentonite fabric is highly compacted, with a tightly-packed arrangement of platy illitic and smectitic clay and mica particles, strongly oriented parallel to bedding (Fig. 5a). Highly altered, shard-like, wispy and “flame-like” particles (up to 500 μm) are common, and are deformed by compaction and elongated parallel to bedding (Fig. 5b). Some of these features preserve a vesicular fabric and probably represent volcaniclastic fragments, mainly pyroclastic fiammè. In addition, siliceous bioclasts (diatoms and sponge spicules) are also present, often in abundance.

The bentonites are extensively affected by diagenetic alteration. The main secondary phases identified are:

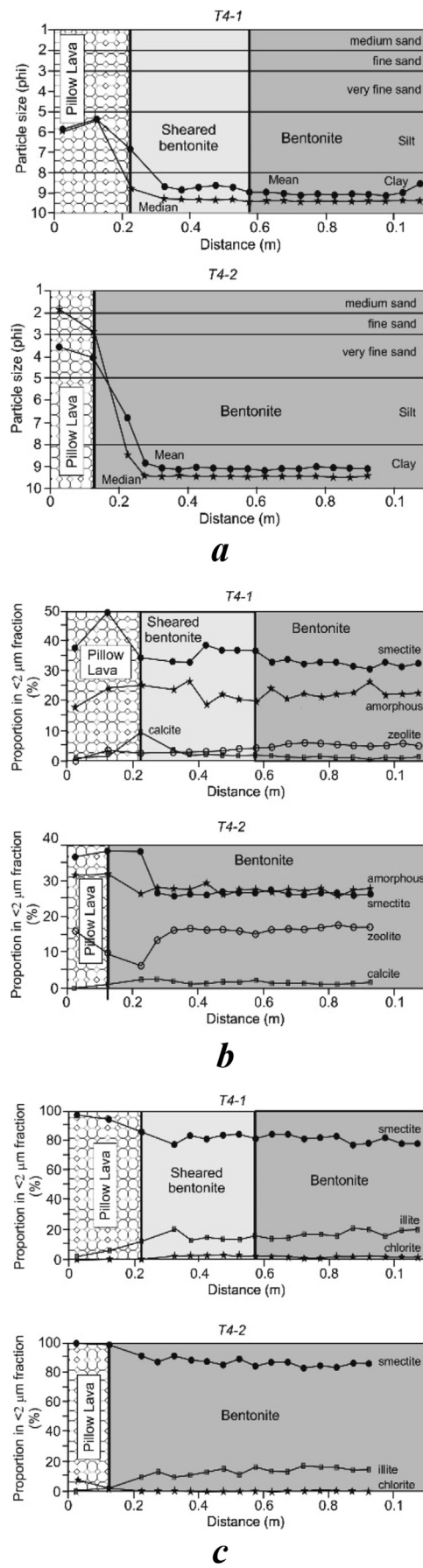
- zeolites, including rare analcite
- amorphous silica
- clay minerals
- calcite
- Ti, Mn and Fe oxides or oxyhydroxides

Detailed SEM analysis reveals that the clay matrix is predominantly tightly cemented by secondary “gelatinous” smectitic material, producing a nanoporous rock with little or no microporosity visible under SEM (Fig. 5a). Zeolites, clay minerals and amorphous silica are the dominant alteration products of the bioclastic detritus and volcaniclastic grains. The clay often forms a matted and fibrous mass and fibrous forms commonly bridge between detrital components. Qualitative and quantitative EDXA analyses of the altered fiammè suggest that the phase is either smectite and/or an Fe-bearing palygorskite (Fig. 6).

EDXA of the ultrafine gelatinous clay matrix is consistent with a predominantly dioctahedral smectite (montmorillonite), although excess silica, possibly due to the presence of amorphous silica, is indicated in many analyses (Fig. 6). Microcrystalline calcite, typically containing minor Mg and Mn, is also dispersed throughout the matrix of some of the mudstone samples. Calcite is also present as patchy cement in secondary pores and as localized fracture fills. Where it has formed in secondary porosity, it encloses and post-dates zeolite mineralization. Fe oxides/hydroxides are commonly associated with altered volcaniclastic particles, locally as fragment rims, and also dispersed through the clay matrix. Ti oxides are similarly dispersed through the clay matrix and as fine crystals within some bioclasts. Dendritic films and small (1–2 mm diameter) nodules of black Mn oxide (probably pyrolusite from bulk XRD analysis) and ochreous goethite are present along bedding planes.

Pervasive, widespread fracturing is present throughout the bentonite as macrofractures with calcite or Fe–Mn oxide mineralization coatings visible to the unaided eye and as microfractures or shear surfaces in the bentonite that are only observable in thin section or under SEM. They commonly run parallel or sub-parallel to lamination (Fig. 5d). Microfractures can also run oblique and perpendicular to lamination. In some cases, microfractures may exist in conjugate pairs. Minor authigenic clay can sometimes be observed as fibrous overgrowths developed from the edges of detrital clay plates and sheets (Fig. 5c). This authigenic clay is best developed on shear planes and microfracture surfaces (Fig. 5c) and was also observed infilling microfractures (Fig. 5d, e). Qualitative EDXA shows that the clay alteration is Mg-rich and probably corresponds to the pervasive palygorskite identified in the bulk XRD analyses (section 4.3). However, the fibrous fracture-mineralizing clay, and associated adjacent altered bentonite wallrock, was too fine to resolve from the montmorillonite clay matrix substrate, and most of the quantitative EDXA data plot around the ideal end-member montmorillonite composition, with some data extending towards a palygorskite-end member (Fig. 6). This would be consistent with the EDXA data representing a mixed analyses of montmorillonite and palygorskite.

Based on examination of mineral replacement and fracture cross-cutting relationships, a paragenetic sequence of diagenetic



alteration and fracture mineralization has been summarised schematically in Fig. 7. In many cases, the relative chronology is unclear or ambiguous and some phases may have formed continuously or during several episodes. The earliest alteration is associated with the dissolution and breakdown of unstable detrital grains, principally glassy volcaniclastic and biogenic silica detritus, probably shortly after deposition. These were replaced by secondary amorphous silica and quartz, zeolites, smectitic clay and fibrous palygorskite.

This early-stage clay alteration is closely associated with impregnation of the sediments by iron and manganese oxides or oxyhydroxides along bedding lamination and microfractures, probably coincident with the formation of early diagenetic manganese micronodules which partially replace the smectitic clay matrix. Later stage fracturing, associated with the localised faulting of the Peripedhi Formation against the UPL, was accompanied by calcite vein mineralization along the fault contact in Trench 4 and in shear-related microfractures in the adjacent hanging wall bentonite (Fig. 3). Early calcite vein mineralization was manganoan, but later microcrystalline calcite mineralization contained little or no Mn. Authigenic fibrous Mg-rich aluminosilicate coats many of these later stage microfracture surfaces and is closely associated with the later microcrystalline calcite. The authigenic clay is restricted to a zone of a few millimetres into the bentonite at the bentonite/UPL contact and to a few micrometres into the matrix of the bentonite behind the face of the fractures. Late-stage goethite coats late dilatational joints in the bentonite and appear to be associated with late-stage fracturing and oxidative alteration that affects the whole bentonite and overlying soil sequence.

#### 4.5. Whole rock chemistry

##### 4.5.1. Major and minor elements

Full details of the whole-rock chemistry of all samples analysed are available in Alexander et al. (2012) and Alexander and Milodowski (2014) and the data are presented in Table S6 (major elements) and S7 (trace elements) in the Supplementary Data. In Trench 4, with the exception of the immediate vicinity of the UPL, there is little systematic lateral variation in composition within the bentonite: CaO is around 2.5%, Na<sub>2</sub>O 1%, Mg 3–4%, K<sub>2</sub>O 1–2%, Al<sub>2</sub>O<sub>3</sub> 12%, SiO<sub>2</sub> 55–62% and Fe<sub>2</sub>O<sub>3</sub> 10%. In the immediate vicinity of the UPL, concentrations generally rise, peaking in the UPL.

In Trench 5, SiO<sub>2</sub> is a little higher with CaO and Fe<sub>2</sub>O<sub>3</sub> lower (<2% and 6%, respectively). The trace elements show no discernible patterns along the transects.

##### 4.5.2. Natural decay series

A useful method of presenting <sup>238</sup>U–<sup>234</sup>U–<sup>230</sup>Th data is in a plot of <sup>234</sup>U/<sup>238</sup>U activity ratio against <sup>230</sup>Th/<sup>238</sup>U activity ratio, which can be divided into uranium deposition and removal sectors corresponding to various continuous, sudden or complex processes (Thiel et al., 1983). Fig. 8 shows such a plot for samples from transect 4-1 (transect 4-2 shows very similar trends).

Natural decay series data from the UPL and the bentonite in Trenches 4 and 5 are presented in Table S8 of the Supplementary Data section. Clearly, the uranium in the rock samples will be a mix of indigenous uranium and uranium deposited on (and in) the solid phases from the groundwater. If groundwater sample P3 is omitted (as there is evidence of ongoing bentonite reaction which is presumably releasing U to the groundwaters, see section 4.1), the

**Fig. 4.** Lateral variation, along the horizontal transects in Trench 4, in the proportion of a) particle size, b) major mineral species in the <2 μm fractions and c) clay minerals (palygorskite excluded) in the <2 μm fractions. Profile 1.

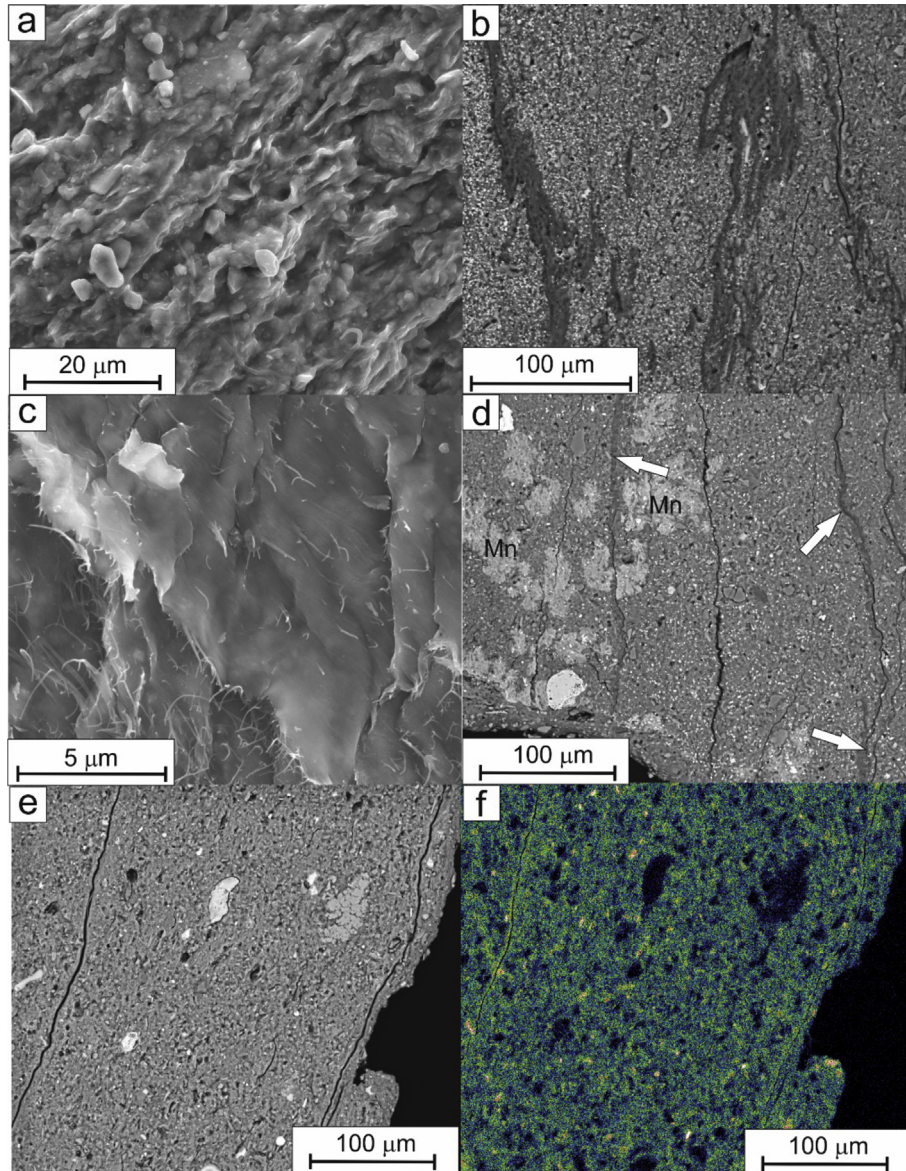


**Fig. 5.** (a) SEM image showing typical bentonite matrix fabric with close-packed sheet-like and platy clay particles, cemented by gelatinous smectitic material (Trench 1); (b) BSEM image showing fiamme textures (defined by darker areas). These are now replaced by authigenic clay with EDXA-derived compositions consistent with smectite and palygorskite (Trench 1); (c) SEM image of a shear microfracture surface showing Mg-rich fibrous authigenic clay growing from the edges of flaky detrital clay particles. The fibrous phase is considered to be palygorskite (Trench 1); (d) BSEM image of bentonite showing microfractures (arrowed) developed parallel to bedding laminae (shown vertical in this image) filled with secondary Mg-rich clay mineralization, considered to correspond to palygorskite based on EDXA. Patchy manganese oxide (Mn) mineralisation impregnates and partly replaces the clay matrix (Trench 4); (e) BSEM image of bentonite from Trench 4, with corresponding EDXA X-ray map (f) showing Mg distribution. Two slightly open microfractures run sub-parallel to the bedding. Texturally, these are marked by 5–10  $\mu\text{m}$  thick bands of smoother clay (A) that coincide with lines of raised Mg in the map (B; green). (For interpretation of the references to colour in this figure legend, the reader is referred to the web version of this article.)

pillow lava ( $^{234}\text{U}/^{238}\text{U} = 1.35 \pm 0.06$ ) and the bentonite samples from the transect 4-1 shear zone ( $^{234}\text{U}/^{238}\text{U} = 1.34 \pm 0.03$  and  $1.28 \pm 0.04$ ) have  $^{234}\text{U}/^{238}\text{U}$  activity ratios (within measurement uncertainty) of the average groundwater value ( $^{234}\text{U}/^{238}\text{U} = 1.36 \pm 0.48$ ).

The general conclusions which can be reached for the data for transects 4-1 and 4-2 (Fig. 8) are that the results show clear evidence of uranium deposition and this is taken here as a proxy for groundwater interaction with the bentonite (cf. Ivanovich and Harmon, 1992) for all samples.

It was hoped that measurement of  $^{226}\text{Ra}$  in the solute and solid phases would provide a finer timescale for the kinetics of reaction than is the case with simply U and Th. However, the low solubility

of Ra in the alkali groundwaters means that  $^{226}\text{Ra}$  was at the limit of detection for all samples. Consequently, errors are large for the  $^{226}\text{Ra}$  data but, despite this, the data indicate that  $^{226}\text{Ra}$  is in secular equilibrium with  $^{230}\text{Th}$  for all of the samples. As such, it can be taken that:

- The equilibrium between  $^{226}\text{Ra}$  and  $^{230}\text{Th}$  indicates that the time since uranium deposition started, or occurred in a single event, is long relative to the  $^{226}\text{Ra}$  half-life ( $1.6 \times 10^3$  years).
- The disequilibrium between  $^{230}\text{Th}$  and  $^{234}\text{U}$  indicates that the uranium deposition has occurred within a time of the same order of magnitude as the  $^{230}\text{Th}$  half-life ( $7.54 \times 10^4$  years).

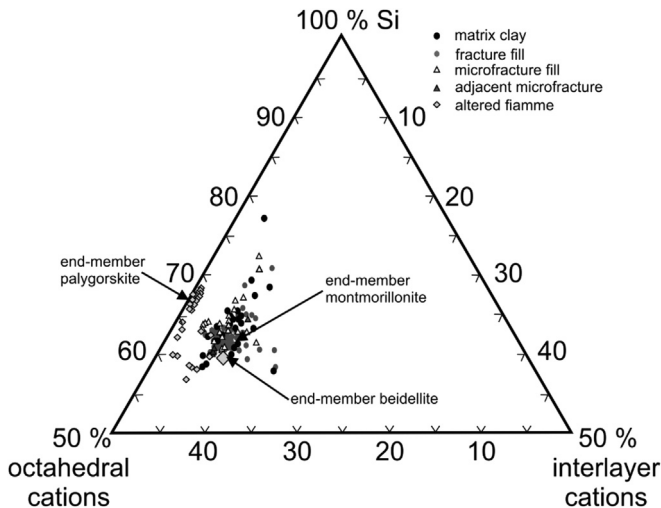


**Fig. 6.** Triaxial plot of atomic ratios of Si-octahedral cations-interlayer cations in clay minerals from samples taken from Trench 4-1 and 4-2 transects (based on quantitative EDXA).

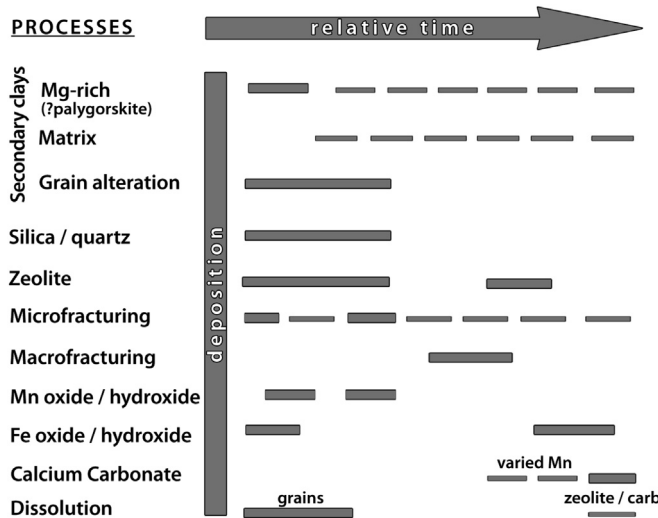


**Fig. 7.** Proposed paragenetic sequence of alteration and mineralization in the bentonite at Parsata (from Alexander and Milodowski, 2014). Broken lines indicate process and mineralization that may have been ongoing, rather than discrete, events.

- If deposition was from groundwater with  $^{234}\text{U}/^{238}\text{U}$  of 1.30, then it occurred on a timescale that is short relative to the  $^{234}\text{U}$  half-life (ca.  $2.45 \times 10^5$  years).

For illustration, if the assumption is made that the uranium in all of the solid phase samples was deposited from the groundwater in a single event with an initial  $^{234}\text{U}/^{238}\text{U}$  activity ratio of 1.3 (see comments above), then the lowest observed solid phase  $^{234}\text{U}/^{238}\text{U}$  activity ratio of  $1.10 \pm 0.03$  would correspond to a time since deposition of approximately  $3.9 \times 10^5$  years (see Scott et al., 1992 for details of the calculation). This approximation provides an indication of the time of initiation of interaction between the uranium in the groundwater and the bulk bentonite, and is supported by trench sample T4-6 ( $^{234}\text{U}/^{238}\text{U} = 1.33$ , Table S8), from just above the UPL, which shows evidence of long-term uranium deposition (once again, see Scott et al., 1992; for details of the calculation) indicating a zone of long-term groundwater-bentonite reaction. This is discussed further in section 5.1.

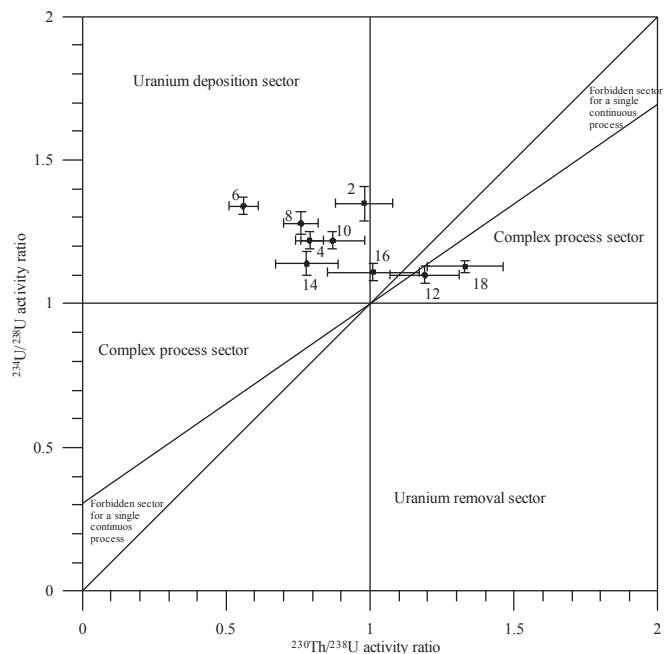


**Fig. 8.** Thiel plot of  $^{234}\text{U}/^{238}\text{U}$  activity ratio against  $^{230}\text{Th}/^{238}\text{U}$  activity ratio for samples from transect T4-1 (see Table S8b for sample details).

#### 4.5.3. Stable isotope and strontium isotope analyses of carbonate mineralization

The  $\delta^{13}\text{C}$  and  $\delta^{18}\text{O}$  and  $^{87}\text{Sr}/^{86}\text{Sr}$  data, for calcite mineralisation filling fine fissures and veins in the bentonite close to the faulted bentonite/UPL contact (transect 4-1) and fissures in the bentonite close to the unconformable bentonite/UPL contact (transect 4-2), are given in Table S8 of the Supplementary Data.

The  $\delta^{13}\text{C}$  and  $\delta^{18}\text{O}$  data for the carbonate minerals and Lefkara Formation chalk clasts are shown cross-plotted in Fig. 9, and are compared with data previously obtained for alkaline spring precipitates from the Allas Springs area of the Troodos which emanate from fresh harzburgite (Alexander et al., 2012). The Parsata calcite mineralisation would appear to fall within the same compositional field as the tufas precipitated from stream waters at Allas Springs which have undergone some degree of reaction with atmospheric  $\text{CO}_2$ .

The Parsata calcite mineralisation is also quite distinct from the marine limestone composition exhibited by the Lefkara Formation chalk clasts, which are obviously isotopically heavier and correspond to what would be expected for marine carbonates. The friable, tufa-like, fissure fills sampled from surface exposures of UPL also appear to form a distinctly different group of carbonates (Fig. 9). They are much heavier, isotopically, and may possibly represent evaporative soil/pedogenic carbonate formation – i.e. calcrete or caliche carbonate. They are quite different to the calcite fracture mineralisation encountered at the base of the bentonite in Trench 4 which, as noted above, lies within the trend in data observed at Allas Springs. This suggests that these samples could have reacted with alkaline groundwater discharging from the underlying UPL along with some intermixing of heavier carbonate from marine chalk clasts observed in the bentonite.

The stable isotope data from Parsata and Allas Springs can be compared to published data for phreatic and alluvial calcite cements associated with the Semal Ophiolite in Oman (Burns and Matter, 1995) where a trend of isotopically lighter carbon is observed in areas with increasing plant activity, and is also observed in areas of increasing rainfall. This would suggest that the

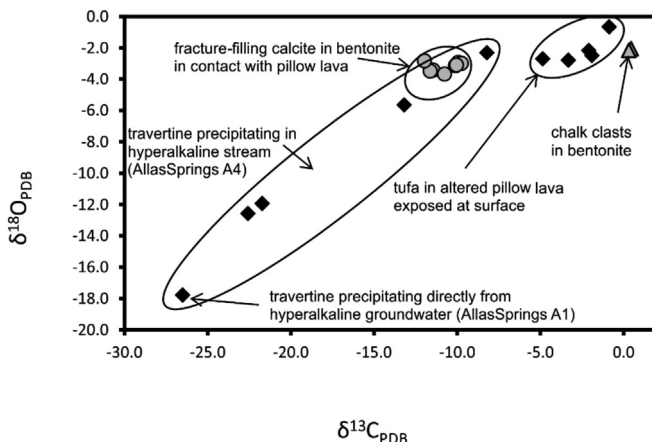


**Fig. 9.** Comparison of stable carbon and oxygen isotope composition of calcite mineralisation from different settings at Parsata, and comparison with active alkaline springs at Allas Springs. (i) Red symbols – data from Alexander et al. (2012) (ii) Blue symbols – calcite mineralisation associated with faulted contact and fine fractures in Peraphedi Formation bentonite close to the contact with UPL, Parsata Trench 4 (this study); (iii) Yellow symbols – typical detrital micritic limestone or chalk clasts of typical Lefkara Formation chalks included within the bentonitic debris flow layer in the top of the sequence in Parsata Trench 4 (this study).

Parsata bentonite-hosted calcite mineralisation is not simply pedogenic carbonate, but that precipitation could result from mixing soil-derived CO<sub>2</sub> (or atmospheric CO<sub>2</sub> dissolved in percolating meteoric water) with a calcium hydroxide-dominated alkaline water discharging into the base of the bentonite from the UPL beneath.

#### 4.5.4. Cation exchange capacity (CEC)

The CEC and exchangeable cation chemistry of samples from the Trench 4 transects are given in Table S7 of the Supplementary Data and plotted in Fig. 10. The bentonite samples from transects 4-1 and 4-2 show generally similar CEC values, ranging from 47 to 59 meq 100 g<sup>-1</sup> (mean ~51 meq 100 g<sup>-1</sup>). The bentonite from Trench 5 displayed slightly lower CEC values, with a mean value of ~39 meq 100 g<sup>-1</sup>, probably reflecting differences in the mineralogy between different sedimentological-stratigraphic horizons in the bentonite.

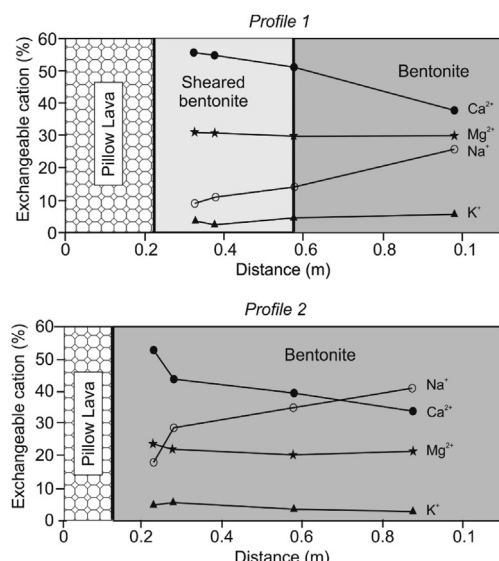


**Fig. 10.** Lateral variation in the exchangeable cation content for samples from Trench 4.

(section 3).

The exchangeable cation chemistry of samples taken along transect 4-1 is generally dominated by divalent Ca and Mg, with minor Na and traces of K. At increasing distance from the contact with the UPL, the proportion of exchangeable Ca decreases with a proportionate increase in Na, while the proportions of Mg and K remain approximately constant. The transect 4-2 exchangeable cation chemistries are also dominated by Ca but, in contrast to the samples from transect 4-1, these samples show higher proportions of Na and subordinate amounts of Mg together with traces of K. However, the transect 4-2 samples show similar trends in exchangeable cation content as the proportion of Ca decreases with a proportionate increase in Na while the proportions of Mg and K remain approximately constant with increasing distance along the transect and away from the UPL source of groundwater. These differences in CEC are not, however, noticeably reflected in the whole rock chemistry (cf. section 4.5.1) or bulk or clay mineralogy (section 4.3).

## 5. Discussion

### 5.1. Groundwater

As noted in sections 2 and 3, the Parsata site was chosen due to evidence for past low-temperature alkali groundwater-bentonite reaction and the current presence of alkali groundwaters in the underlying UPL (e.g. borehole P1 groundwater). This was supported by the resistivity survey of the site which indicated the presence of groundwaters at shallow depth immediately below the bentonite, leading to the excavation of Trenches 1 and 4 down to the surface of the UPL.

Although the bottoms of the trenches were damp, no flowing groundwater was encountered, but the stable isotope data (section 4.2.3) indicate water-bentonite interaction. The <sup>87</sup>Sr/<sup>86</sup>Sr ratios suggest reaction with a groundwater which has a mixed signature, composed predominantly of alkaline groundwaters but with a signature of material probably derived from the overlying bentonite. Several aspects of the groundwater signature from borehole P3 (section 4.1) also suggest alkali groundwater-bentonite interaction.

This is further supported by the CEC data (section 4.5.4) which indicate Ca exchange onto the Na bentonite, just as would be expected when a Ca(OH)<sub>2</sub> dominated alkali groundwater of the type found in borehole P1 (section 4.1) would react with the base of the bentonite. There is an overall change from Na-dominated exchangeable cation chemistry in the Trench 5 bentonite (far from the alkali groundwaters in the UPL) to Ca-dominated exchangeable cation chemistry in the bentonite in Trench 4. The Ca levels are highest near the UPL, consistent with a model whereby Ca(OH)<sub>2</sub>-rich groundwater penetrates the bentonite from the underlying UPL sequence, with Ca exchange displacing Na in the original bentonite.

Although the data are limited (both statistically and spatially), the effect of cation-exchange through interaction with this Ca-rich groundwater appears to extend for a distance of at least 0.1 m from the contact, but note that the exchangeable cation chemistry does not approach a similar composition to that of the bentonite far from the UPL (as represented in Trench 5) and it is therefore assumed that the CEC 'front' penetrates much further into the bentonite. That biogenic silica is still present throughout the bentonite, despite being unstable at high pH (e.g. Loucaides et al., 2008, 2012) is simply a question of mass balance: at the exchangeable cation levels observed in the bentonite, no more than 0.05% of the biogenic silica is likely to have dissolved during penetration of the high pH front.

Finally, the uranium series disequilibria results (section 4.5.2) imply initiation of groundwater/rock interaction at the base of the bentonite in the last  $10^4$ – $10^6$  years,<sup>3</sup> with rock–groundwater reaction ongoing today in some zones. This timespan for groundwater/rock reaction are supported by an independent analysis (Pitty et al., 2012) of the island-wide (with focus on Parsata) geomorphological evolution over the last 1 Ma. This indicated that low-temperature serpentinisation reactions (producing the alkali groundwaters sampled in the UPL) were probably initiated in the last  $10^5$ – $10^6$  years.

Palaeoclimatic studies show that alternating humid and more arid conditions (ca. every 21 ka in the eastern Mediterranean; Pitty et al., 2012) are endemic in this area and are primarily forced by solar precession. This means that, although groundwater flow at the base of the bentonite has probably not been continuous, alkali groundwater appears to be present today, despite the decade-long drought currently affecting the island and the significant drawdown of groundwater tables in the last half century through over-extraction. In addition, as noted by Wilson et al. (2011) "... due to the high chemical suctions for water in partially saturated bentonite, water will tend to be drawn in from the surrounding host rock into the bentonite." As can be seen from Table S2 in the Supplementary Data, the Parsata bentonite is only partially saturated at present and so is likely drawing in available groundwater (as implied by the natural decay series data, section 4.5.2). As such, although it has not yet proven possible to measure groundwater fluxes at the base of the bentonite, it appears that any reaction of the bentonite should not have been limited by supply of reactants from the groundwater.

## 5.2. Bentonite reaction products

Despite this evidence for groundwater-bentonite reaction, XRD analysis (section 4.3) of the bentonite clay mineral fraction revealed no evidence of denaturing or decomposition of the montmorillonite components. However, detailed SEM petrographic observations (section 4.4) identified a secondary Mg-rich fibrous clay mineral, with a palygorskite-like (or Fe-rich palygorskite) composition, to be forming on the surfaces of reacting, sheet-like montmorillonite particles (Fig. 5c). The SEM revealed that the surface layers of montmorillonite particles were exfoliating and breaking down to form the fibrous secondary Mg-rich silicate phase.

Palygorskite requires alkaline conditions and high Si and Mg activities for stability (e.g. Weaver and Beck, 1977; Hojati et al., 2010). Palygorskite can also be formed by pedogenic processes, and is found as an authigenic mineral under evaporative conditions, often associated with calcrete formation, in arid environment soils and palaeosols (e.g. Galan and Singer, 2011). It is also formed in highly saline, playa and alkaline lake sediments (e.g. Singer, 1991; Bristow and Milliken, 2011), where it may also form as an alteration product of smectite. Formation in these environments appears to be favoured by the alkaline conditions and high concentration of Mg. The destabilisation of smectite and its breakdown to palygorskite in saline/alkaline lake environments is also encouraged by increasing Mg:Ca ratios in the porewater (Botha and Hughes, 1992; Chen et al., 2004). Palygorskite can also precipitate directly from groundwaters with high Mg and Si activities (e.g. Singer and Galan, 1984; Hojati et al., 2010), but the textural relations observed in the Parsata samples (section 4.4) would appear to rule this out here.

Palygorskite can also transform to smectite over several months (Galan and Singer, 2011), but requires buffering the solute pH to  $\geq 12$  (e.g. Golden and Dixon, 1990). Certainly, none of the textural evidence from the Parsata samples indicates palygorskite transformation to smectite and the (admittedly limited) hydrochemical data would not support such high *in situ* pH levels during reaction.

The presence of palygorskite in the bentonites of southern Cyprus has been reported previously by Gass et al. (1994). Christidis (2006) also described partial replacement of smectite by fibrous palygorskite in these deposits and this was attributed to the interaction of the smectite with Si-rich porewaters produced by the dissolution of abundant siliceous radiolarian frustules by the circulation of hydrothermal fluids. This is presumably a relatively early event and therefore unlikely to be associated with the late-stage palygorskite observed here (section 4.4). However, dissolution of the amorphous and poorly-crystalline biogenic (radiolarian) silica present in the Peripedhi bentonite could occur by interaction with alkaline groundwater (cf. Loucaides et al., 2012), to produce high-Si porewaters that would then lead to smectite alteration.

## 5.3. Reaction times

While the  $10^4$ – $10^6$  years reaction timescale (but see footnote 3) of this study is directly relevant to repository conditions, other work might imply that this could be an upper estimate of the reaction times. For example, Hillier and Pharande (2008) note that changing field water management in Maharashtra, India, from simple precipitation to an irrigation scheme produced saline-sodic soils rich in secondary palygorskite (from smectite) in just 40–50 years, "... implying that palygorskite formation in the irrigated, saline-sodic soils has been an extremely rapid process."

Further, recent mineralogical studies (Moyle et al., 2014) have identified palygorskite- and sepiolite-like fibrous Mg-rich silicates as alteration products in medium-term (15 years) laboratory batch experiments examining the interaction of "young" (K, Na-rich) and "evolved" (Ca-rich) alkaline cement porefluids with rock from the Sellafield area of the UK. The original experimental study (Rochelle et al., 1997) reported that, after 2 years, cement phases such as amorphous calcium silicate hydrate (CSH), ettringite and possibly apophyllite were produced as reaction products that originally replaced clay mineral or other phyllosilicates. The more recent mineralogical observations have shown that the early-formed CSH, ettringite and possible apophyllite reaction products are no longer present, dolomite has been extensively dissolved and partially-replaced by calcite and the silicate reaction products are now dominated by a palygorskite-like Mg-rich silicate. The pH of the reacting fluid has now been buffered (presumably by reaction with the rock) down to  $<9$  – as observed in the P3 borehole.

However, these examples of fast reaction of smectite should not be over-interpreted: the flux of reactants (in the former study) and the reactant:clay ratio (in the latter) are vastly different from the likely repository environment where a very low flux of groundwaters (and, therefore, alkali leachates) is expected and where the alkali leachate:bentonite ratio will be massively smaller (see, for example, Chapman et al., 2009). As such, the results of the Cyprus study are much more relevant to the repository environment than either of these examples.

That there has been very limited alteration of the bentonite over a period of  $10^5$ – $10^6$  years in Cyprus tends to indicate that any long-term bentonite reaction in low alkali cement leachates in a repository could be minimal. This may be attributed, at least in part, to 'self-armouring' of the bentonite as it naturally swells when encountering water (although it does not appear to be due the 'cement armouring' reported by Fernandez et al., 2009). This emphasises the fact that (as noted above) any similar NA study of

<sup>3</sup> However, due to the large uncertainties on the  $^{226}\text{Ra}$  data, little weight can be placed on the lower age, meaning  $10^5$ – $10^6$  years is more likely (as supported by the geomorphological study).

bentonite longevity must also take into account physical scales so that the study conditions approach those of a repository as closely as possible as only then will the latent physico-chemical behaviour of the bentonite be observed (see also Alexander et al., 2014; for discussion).

#### 5.4. Comparison with other studies

Laboratory and modelling studies of cementitious alkaline fluid–bentonite reaction (e.g. Metcalfe and Walker, 2004) generally indicate that the calcium-rich fluids will exchange with the bentonite (as seen here, section 4.5.4) and be incorporated into smectite alteration products such as Ca-zeolites, CSH and CASH phases. For example, recent work from the advective system at Searles Lake (Savage et al., 2010b) reports different reaction products and claim smectite susceptibility to alter from pH 9 upwards, but the authors acknowledge that this is in a system which is far from the low flux, diffusion dominated system expected in a repository. Further, scoping calculations (J. Wilson, *pers comm.*, 2014) of the Parsata system solute speciation using PHREEQC (Parkhurst and Appelo, 1999) and the Lawrence Livermore ‘LLNL.dat’ thermodynamic database, could only induce palygorskite formation under very high dissolved silica activities. As such, the difference between the Parsata system and others studied to date appears to be two-fold:

- Although the P1 input groundwaters are low Mg in absolute terms ( $0.04 \text{ mgL}^{-1}$ ), they nevertheless are oversaturated with respect to antigorite (Mg-rich, serpentine-like mineral), effectively saturated with respect to brucite ( $\text{Mg(OH)}_2$ ), undersaturated with respect to montmorillonite, beidellite and quartz and oversaturated with respect to saponite (J. Wilson, *pers comm.*, 2014).
- Thermodynamic data (e.g. Birsoy, 2002) and mineralogical observations from the other natural occurrences noted above suggest that palygorskite is only stable under very high dissolved silica activities.

The Parsata findings could therefore be taken to be non-representative of repository systems, but this is somewhat over-simplistic. For example, Fernandez et al. (2009) Mg-exchanged the La Serrata processed bentonite and subsequent interaction with alkali fluids produced Mg-silicate reaction products (brucite, Mg-smectite and a chlorite-like phase). While the above scenario is unlikely in a repository, it should be possible to produce Mg-smectites where a potential repository site has sufficient Mg levels in the groundwaters: for example the groundwaters at the Forsmark site in Sweden show a range of  $0.1\text{--}448 \text{ mgL}^{-1}$  Mg (Laaksoharju, 2005) while the porewaters of the Opalinus Clay in Switzerland have a range of  $430\text{--}800 \text{ mgL}^{-1}$  Mg (Bradbury and Baeyens, 1998). Indeed, other laboratory studies of the interaction of cement fluids with clays have reported a range of Mg silicate reaction products (e.g. Ramirez et al., 2002; Dauzeres et al., 2014) and, where low alkali cement leachates are concerned, the reaction products have been described as poorly crystallized magnesium silicate hydrate phases (cf. Roosz et al., 2015).

It also seems unlikely that the Mg content of the Peripedhi bentonite could have contributed to the production of palygorskite. Samples from transects 4-1 and 4-2 have a range in MgO content of 3.04–4.43% (1.55–2.19% for T5), levels which are well within the 1.93–5.10% range for 17 processed bentonites (including MX80) noted by Kumpulainen and Kiviranta (2010) and Kiviranta and Kumpulainen (2011).

At Parsata, the high levels of amorphous silica (and relict glass) present (section 4.4) have presumably dissolved (at least locally) in

the high pH groundwaters from the underlying UPL (cf. section 5.2), producing the high silica activities required for palygorskite stability (as noted in the thermodynamic scoping calculations). High dissolved silica activities are not to be expected in most processed bentonites as the beneficiation of the clay increases the smectite content at the cost of the other components originally present in the natural bentonite. However, typical requirements (e.g. Posiva, 2013) for processed bentonite for repositories require only >75% smectite and provide no limits for the accessory minerals, so high silica activities may not be out-of-the-question. In addition, as more repository designs move towards implementation, processed bentonite is being mixed with silica sand or the local repository host rock, to produce a mix with higher silica levels, so changing the currently assumed boundary conditions.

Unfortunately, models of bentonite reaction (e.g. Savage and Benbow, 2007; Lehikoinen, 2009) do not currently include the dissolution of silica sand, amorphous materials and/or glasses, assuming instead only processed bentonite (i.e. smectite with minor, inert, accessory phases) will be present. The results reported here suggest that this may be an oversight which should be addressed in the near future.

#### 6. Conclusions

The results of the analyses which are presented here suggest that there has been very limited alkaline groundwater reaction with the natural bentonite over a period of  $10^4\text{--}10^6$  years (with greater certainty placed on the  $10^4\text{--}10^6$  period), tending to indicate that any long-term reaction of processed bentonite with low alkali cement leachates in a repository environment will be minimal. This adds weight to arguments supporting the use of low alkali cements for structural concrete, roadways, tunnel seals, shaft plugs etc in repositories for high-level radioactive waste and spent fuel which envisage using large volumes of bentonite to encapsulate the waste packages (see Alexander and McKinley, 2007; for details). Perhaps of equal importance is the fact that, when compared with most existing NA, laboratory and URL studies of bentonite reaction in alkali solutes, this is the first to approach repository conditions (see also comments in Reijonen and Alexander, 2015) insofar that the field conditions closely simulate what would be expected in a repository:

- an appropriately large mass of bentonite is ‘in place’, rather than a small plug within laboratory apparatus
- an appropriate alkali leachate can react with the surface of the bentonite in a manner similar to what would be expected in the repository, rather than in the unrealistic conditions (e.g. inappropriate bentonite:leachate ratio) common in laboratory and previous natural system studies
- reaction between the leachate and the bentonite appears to be generally driven by diffusive transport of solutes (especially Ca) into the body of the bentonite from the bentonite/alkali leachate contact zone, again as would be expected in a repository
- the temperatures of reaction are also repository relevant
- the reaction timescales are of much more relevance to a repository than accelerated laboratory and URL studies

Overall, it is these physical and temporal similarities between the natural bentonite/ophiolite groundwater environment and that expected for processed bentonite in a repository exposed to low alkali cement leachates which argues most strongly for limited reaction in the repository environment. That Mg-silicate reaction phases have not been considered in previous waste disposal studies is simply a reflection of the limited range of repository EBS designs and host rock types examined to date. In any case, the precise

nature of the secondary phase may well prove less important to the long-term performance of the repository than the limited extent of alteration of the bentonite which points to an EBS which is robust enough to survive for the timescales of concern to the repository safety assessment.

## Acknowledgements

The authors would like to thank their colleagues at BGS (UK), in particular Simon Kemp (XRD analyses) and Jeremy Rushton (petrography), SUERC (UK) and Terra Marine (Greece) for their support. Particular thanks go to Mr Andreas Siathas (Geoinvest, Cyprus) and Mr Michael Rigas and his colleagues at the GSD (Cyprus) for their unstinting help, recommendations and advice throughout the duration of this project. Thanks also to Prof Alistair Pitty (Pitty (EIA) Consulting, UK), Dr Petri Korkeakoski (Posiva, Finland) and Dr Patrik Sellin (SKB, Sweden). The financial support of the three Project Partners, RWM Ltd (UK), Posiva (Finland) and SKB (Sweden) is gratefully acknowledged. AEM publishes with the permission of the Executive Director of the British Geological Survey (NERC). The authors also thank the handling editor and two anonymous reviewers for constructive comments which have improved the clarity of the original manuscript.

## Appendix A. Supplementary data

Supplementary data related to this article can be found at <http://dx.doi.org/10.1016/j.apgeochem.2015.12.016>.

## References

- Ahokas, H., Hellä, P., et al., 2006. Control of Water Inflow and Use of Cement in ONKALO after Penetration of Fracture Zone R19. Posiva Working Report 2006-45. Posiva, Olkiluoto, Finland.
- Ahonen, L., Korkeakoski, P., Tijander, M., Kivikoski, H., Laaksonen, R., 2008. Quality Assurance of the Bentonite Material. Posiva Working Report WR2008-33. Posiva, Eurajoki, Finland.
- Alexander, W.R., 1985. Inorganic Diagenesis in Anoxic Sediments of the Tamar Estuary. PhD Thesis. University of Leeds, 268pp.
- Alexander, W.R., Neall, F.B., 2007. Assessment of Potential Perturbations to Posiva's SF Repository at Olkiluoto Caused by Construction and Operation of the ONKALO Facility. Posiva Working Report 2007-35. Posiva, Olkiluoto, Finland.
- Alexander, W.R., McKinley, L.E. (Eds.), 2007. Deep Geological Disposal of Radioactive Wastes. Elsevier, Amsterdam, The Netherlands.
- Posiva Working Report WR 2011-08. In: Alexander, W.R., Milodowski, A.E. (Eds.), 2011. Cyprus Natural Analogue Project (CNAP) Phase II Final Report. Posiva, Eurajoki, Finland.
- Posiva Working Report WR 2014-02. In: Alexander, W.R., Milodowski, A.E. (Eds.), 2014. Cyprus Natural Analogue Project (CNAP) Phase IV Final Report. Posiva, Eurajoki, Finland.
- Alexander, W.R., Gautschi, A., Zuidema, P., 1998. Thorough testing of performance assessment models: the necessary integration of *in situ* experiments, natural analogues and laboratory work. *Sci. Basis Nucl. Waste Manag.* XXI, 1013–1014.
- Alexander, W.R., Arcilla, C.A., McKinley, I.G., Kawamura, H., Takahashi, Y., Aoki, K., Miyoshi, S., 2008. A new natural analogue study of the interaction of low-alkali cement leachates and the bentonite buffer. *Sci. Basis Nucl. Waste Manag.* XXXI, 493–500.
- Posiva Working Report WR 2011-77. In: Alexander, W.R., Milodowski, A.E., Pitty, A.F. (Eds.), 2012. Cyprus Natural Analogue Project (CNAP) Phase III Final Report. Posiva, Eurajoki, Finland.
- Alexander, W.R., Milodowski, A.E., Pitty, A.F., Hardy, S.M.L., Kemp, S.J., Rushton, J.C., Siathas, A., Siathas, A., Mackenzie, A.B., Korkeakoski, P., Norris, S., Sellin, P., Rigas, M., 2013. Bentonite reactivity in alkaline solutions: interim results of the Cyprus Natural Analogue Project (CNAP). *Clay Mineral.* 48, 235–249.
- Alexander, W.R., McKinley, I.G., Kawamura, H., 2014. The process of defining an optimal natural analogue programme to support national disposal programmes. In: Proc. NEA-GRS Workshop on Natural Analogues for Safety Cases of Repositories in Rock Salt. 4 – 6 September, 2012, Braunschweig, Germany. NEA/OECD, Paris, France.
- Alexander, W.R., Reijonen, H.M., McKinley, I.G., 2015. Natural analogues: studies of geological processes relevant to radioactive waste disposal in deep geological repositories. *Swiss J. Geosci.* 108, 75–100.
- Bear, J.M., 1960. The geology and mineral resources of the Akaki-Lythrondondha area. In: Geological Survey Department Memoirs No. 3GSD, Lefkosa, Cyprus.
- Birsoy, R., 2002. Formation of sepiolite-palygorskite and related minerals from solution. *Clays Clay Minerals* 50, 736–745.
- Boronina, A.V., 2003. Application of Numerical Modelling, Isotope Studies and Streamflow Observations for Quantitative Description of Hydrogeology of the Kouris Catchment (Cyprus). ETH PhD Thesis No. 15338. ETH (Swiss Federal Institute of Technology), Zürich, Switzerland.
- Boronina, A.V., Balderer, W., Renard, P., Stichler, W., 2005. Study of stable isotopes in the Kouris catchment (Cyprus) for the description of the regional groundwater flow. *J. Hydrol.* 308, 214–226.
- Botha, G., Hughes, J.C., 1992. Pedogenic palygorskite and dolomite in a late Neogene sedimentary succession, northwestern Transvaal, South Africa. *Geoderma* 53, 139–154.
- Bradbury, M.H., Baeyens, B., 1998. Derivation of *in Situ* Opalinus Clay Porewater Compositions from Experimental and Geochemical Modelling Studies. Nagra Technical Report NTB97-07. Nagra, Wettingen, Switzerland.
- Bristow, T.F., Milliken, R.E., 2011. Terrestrial perspective on authigenic clay mineral production in ancient Martian lakes. *Clay Clay Mins* 59, 339–358.
- Burns, S.J., Matter, A., 1995. Geochemistry of carbonate cements in surficial alluvial conglomerates and their paleoclimatic implications, Sultanate of Oman. *J. Sediment. Res.* A65, 170–177.
- Chapman, N.A., Baldwin, T., Neall, F.B., Mathieson, J., White, M., 2009. Design options for the UK's HLW geological disposal facility. *Radwaste Solut.* 16, 44–54.
- Chen, T., Xu, H., Lu, A., Xu, X., Peng, S., Yue, S., 2004. Direct evidence of transformation of smectite to palygorskite: TEM investigation. *Sci. China Ser. D Earth Sci.* 47, 985–994.
- Christidis, G.E., 2006. Genesis and compositional heterogeneity of smectites. Part III: alteration of basic pyroclastic rocks—A case study from the Troodos Ophiolite Complex, Cyprus. *Am. Min.* 91, 685–701.
- Davies, E.E., Elderfield, H. (Eds.), 2004. Hydrogeology of the Oceanic Lithosphere. Cambridge University Press, Cambridge, UK.
- Dauzères, A., LeBescop, P., Cau-Dit-Coumes, C., Brunet, F., Bourbon, X., Timonen, J., Voutilainen, M., Chomat, L., Sardini, P., 2014. On the physico-chemical evolution of low-pH and CEM I cement pastes interacting with Callovo-Oxfordian pore water under its *in situ* CO<sub>2</sub> partial pressure. *Cem. Concr. Res.* 58, 76–88.
- Fernandez, R., Mäder, U.K., Rodriguez, M., Vigil de la Villa, R., Cuevas, J., 2009. Alteration of compacted bentonite by diffusion of highly alkaline solutions. *Eur. J. Miner.* 21, 725–735.
- Fujita, K., Sato, T., Nakabayashi, R., Yamakawa, M., Fujii, N., Namiki, K., Pascua, C., Arcilla, C., Alexander, W.R., Yoneda, T., 2010. Natural analogue study of the interaction between hyperalkaline groundwater and bentonite at the ophiolite of Philippine. In: Proc. Japan Geoscience Union Meeting, 23–28 May, 2010, Makuhari, Japan. JGU, Tokyo, Japan (in Japanese).
- Galan, E., Singer, A. (Eds.), 2011. Developments in Palygorskite – Sepiolite Research: a New Outlook on These Materials. Developments in clay sciences 3, Elsevier, Amsterdam, The Netherlands.
- Gass, I.D., MacCleod, C.J., Murton, B.J., Panayiotou, A., Simonian, K.O., Xenophontos, C., 1994. The Geology of the Southern Troodos Transform Fault Zone. In: Geological Survey Department Memoir No.9. GSD, Lefkosa, Cyprus.
- Golden, D.C., Dixon, J.B., 1990. Low temperature alteration of palygorskite to smectite. *Clay Clay Mins* 38, 401–408.
- Haworth, A., Sharland, S.M., Tasker, P.W., Tweed, C.J., 1987. Evolution of the groundwater chemistry around a nuclear waste repository. *Sci. Basis Nucl. Waste Manag.* XI, 425–434.
- Heikola, T., Kumpulainen, S., Vuorinen, U., Kiviranta, L., Korkeakoski, P., 2013. Influence of alkaline and saline solutions on chemical, mineralogical and physical properties of two different bentonites – batch experiments at 25 °C. *Clay Mins* 48, 309–329.
- Hillier, S., Pharande, A.L., 2008. Contemporary pedogenic formation of palygorskite in irrigation-induced saline-sodic, shrink-swell soils of Maharashtra, India. *Clay Clay Mins* 56, 531–548.
- Hojati, S., Khademi, H., Cano, A.F., 2010. Palygorskite formation under the influence of groundwater in central Iranian soils. *Anadolu Tarım Bilim. Derg.* 25 (S-1), 34–41.
- Ishikawa, T., Nakamura, E., 1993. Boron isotope systematics of Marine sediments. *Earth Planet. Sci. Lett.* 117, 567–580.
- Ivanovich, M., Harmon, R.S. (Eds.), 1992. Uranium-series Disequilibrium: Applications to Earth, Marine, and Environmental Sciences, second ed. Oxford Science Publications, Oxford, UK.
- Kiviranta, L., Kumpulainen, S., 2011. Quality Control and Characterization of Bentonite Materials. Posiva Working Report WR 2011-84. Posiva, Eurajoki, Finland.
- Kreitler, C.W., Bledsoe, B.E., 1993. Geochemical Techniques for Identifying Sources of Ground-water Salinization. CRC Press, London, UK.
- Kumpulainen, S., Kiviranta, L., 2010. Mineralogical and chemical characterization of various bentonite and smectite-rich Clay materials. Posiva Working Report WR 2010-52. Posiva, Eurajoki, Finland.
- Kunimaru, T., Ota, K., Alexander, W.R., Yamamoto, H., 2011. Hydrochemistry of the Groundwaters from JAEA's Horonobe URL: Data Freeze II - Preliminary Evaluation of Boreholes HDB1 to HDB8 and Field Manual for On-site Practices. JAEA Report 2011-010. JAEA, Tokai, Japan.
- SKB Report R 05-17, Stockholm, Sweden. In: Laaksoharju, M. (Ed.), 2005. Hydrogeochemical Evaluation of the Forsmark Site, Model Version 1.2. Preliminary Site Description of the Forsmark Area.
- Lehikoinen, J., 2009. Bentonite-cement Interaction –Preliminary Results from Model Calculations. Posiva Working Report WR 2009-37. Posiva, Eurajoki, Finland.

- Linklater, C.M., Albinsson, Y., Alexander, W.R., Casas, I., McKinley, I.G., Sellin, P., 1996. A natural analogue of high pH cement pore waters from the Maqrin area of northern Jordan: comparison of predicted and observed trace element chemistry of uranium and selenium. *J. Contam. Hydrol.* 21, 59–69.
- Loucaides, S., Van Cappellen, P., Behrends, T., 2008. Dissolution of biogenic silica from land to ocean: role of salinity and pH. *Limnol. Ocean.* 53, 1614–1621.
- Loucaides, S., Van Cappellen, P., Roubeix, V., Moriceau, B., Ragueneau, O., 2012. Controls on the recycling and preservation of biogenic silica from biomineralization to burial. *Silicon* 4, 7–22.
- McKinley, I.G., Alexander, W.R., Blaser, P.C., 2007. Development of geological disposal concepts. Ch. 3. In: Alexander, W.R., McKinley, L.E. (Eds.), Deep Geological Disposal of Radioactive Wastes. Elsevier, Amsterdam, The Netherlands.
- Metcalfe, R., Walker, C., 2004. In: Proceedings of the International Workshop on Bentonite-cement Interaction in Repository Environments 14–16 April 2004, Tokyo, Japan. NUMO-TR-04-05, NUMO, Tokyo, Japan. NUMO Tech. Rep.
- Miller, W.M., Alexander, W.R., Chapman, N.A., McKinley, I.G., Smellie, J.A.T., 2000. Geological Disposal of Radioactive Wastes and Natural Analogues. In: Waste Management Series, vol. 2. Pergamon, Amsterdam, The Netherlands.
- Moyce, E.B.A., Rochelle, C.A., Morris, K., Milodowski, A.E., Chen, X., Thornton, S., Small, J.S., Shaw, S., 2014. Rock alteration in alkaline cement waters over 15 years and its relevance to the geological disposal of nuclear waste. *Appl. Geoch.* 50, 91–105.
- NDA, 2010. Geological Disposal: Geosphere Status Report. NDA Report No. NDA/RWMD/035. RWM Ltd, Harwell, UK.
- Neal, C., Shand, P., 2002. Spring and surface water quality of the Cyprus Ophiolites. *Hydrol. Earth Syst. Sci.* 6, 797–817.
- Parkhurst, D.L., Appelo, C.A.J., 1999. User's Guide to PHREEQC (Version 2). A Computer Program for Speciation, Batch-reaction; One-dimensional Transport and Inverse Geochemical Calculations. US Geological Survey Water Resources Investigations Report, pp. 99–4259.
- Pitty, A.F., Milodowski, A.E., Alexander, W.R., 2012. Geomorphology (chapter 3). In: Alexander, W.R., Milodowski, A.E., Pitty, A.F. (Eds.), Cyprus Natural Analogue Project (CNAP) Phase III Final Report. Posiva, Eurajoki, Finland. Posiva Working Report WR 2011-77.
- Posiva, 2013. Safety Case for the Disposal of Spent Nuclear Fuel at Olkiluoto –Description of the Disposal System 2012. Posiva Report R 2012-05. Posiva, Eurajoki, Finland.
- Ramirez, S., Cuevas, J., Vigil, R., Leguey, S., 2002. Hydrothermal alteration of "La Serrata" bentonite (Almeria, Spain) by alkaline solutions. *Appl. Clay Sci.* 21, 257–269.
- Reijonen, H.M., Alexander, W.R., 2015. Bentonite analogue research related to geological disposal of radioactive waste – current status and future outlook. *Swiss J. Geosci. Special Issue* 108, 101–110.
- Reynolds, R.C., Reynolds, R.C., 1996. Description of Newmod-for-windows™. The Calculation of One-dimensional X-ray Diffraction Patterns of Mixed Layered Clay Minerals. R.C.Reynolds Jr., 8 Brook Road, Hanover, USA.
- Rochelle, C.A., Pearce, J.M., Bateman, K., Coombs, P., Wetton, P.D., 1997. The Evaluation of Chemical Mass Transfer in the Disturbed Zone of a Deep Geological Disposal Facility for Radioactive Wastes. X: Interaction between Synthetic Cement Porefluids and BVG: Observations from Experiments of 4, 9 and 15 Months Duration. British Geological Survey (BGS), Fluid Processes and Waste Management Group Report, WE/97/16C, 79p. BGS, Keyworth, UK.
- Roosz, C., Grangeon, S., Blanc, P., Montouillout, V., Lothenbach, B., Henocq, P., Giffaut, E., Vieillard, P., Gaboreau, S., 2015. Crystal structure of magnesium silicate hydrates (M-S-H): the relation with 2:1 Mg–Si phyllosilicates. *Cem. Concr. Res.* 73, 228–237.
- Savage, D., Benbow, S., 2007. Low PH Cements. SKI report 2007:32. SSM (Swedish Nuclear Power Inspectorate), Stockholm, Sweden.
- Savage, D., Arthur, R., Watson, C., Wilson, J., 2010a. An Evaluation of Models of Bentonite Pore Water Evolution. Swedish Radiation Safety Authority (SSM) Report 2010-12. SSM, Stockholm, Sweden.
- Savage, D., Benbow, S., Watson, C., Takase, H., Ono, K., Oda, C., Honda, A., 2010b. Natural systems evidence for the alteration of clay under alkaline conditions: an example from Searles Lake, California. *Appl. Clay Sci.* 47, 72–81.
- Scott, R.D., MacKenzie, A.B., Alexander, W.R., 1992. The interpretation of  $^{238}\text{U}$ - $^{234}\text{U}$ - $^{230}\text{Th}$ - $^{226}\text{Ra}$  disequilibria produced by rock-water interaction. *J. Geochim. Explor.* 46, 323–343.
- Sidborn, M., Marsic, N., Crawford, J., Joyce, S., Hartley, L., Idiart, A., de Vries, L.M., Maia, F., Molinero, J., Svensson, U., Vidstrand, P., Alexander, W.R., 2015. Potential Alkaline Conditions for Deposition Holes of a Repository in Forsmark as a Consequence of OPC Grouting. SKB R-12–17, SKB, Stockholm, Sweden.
- Singer, A., 1991. Polygorskite in sediments: detrital, diagenetic or neoformed – a critical review. *Geol. Rundsch.* 68, 996–1008.
- Singer, A., Galan, E. (Eds.), 1984. Polygorskite – Sepiolite: Occurrences, Genesis and Uses. Developments in Sedimentology. Elsevier, Amsterdam, The Netherlands.
- Soler, J.M., Vuorio, M., Hautajarvi, A., 2011. Reactive transport modelling of the interaction between water and a cementitious grout in a fractured rock. Application to ONKALO (Finland). *Appl. Geochim.* 26, 1115–1129.
- Thiel, K., Vorwerk, R., Saager, R., Stupp, H.D., 1983.  $^{235}\text{U}$  fission tracks and  $^{238}\text{U}$ -series disequilibria as a means to study recent mobilization of uranium in Archaean pyritic conglomerates. *Earth Planet. Sci. Lett.* 65, 249–262.
- Truscott, M.G., Shaw, D.M., 1984. Boron in chert and precambrian siliceous iron formations. *Geochim. Cosmochim. Acta* 48, 2313–2320.
- Vuorinen, U., Lehikoinen, J., Imoto, H., Yamamoto, T., Alonso, M.C., 2005. Injection Grout for Deep Repositories. Subproject 1: Low PH Cementitious Grout for Larger Fractures, Leach Testing of Grout Mixes and Evaluation of the Long-term Safety. Posiva Working Report 2004-46. Posiva, Eurajoki, Finland.
- Weaver, C.E., Beck, K.C., 1977. Miocene of S.E. United States: a model for chemical sedimentation in a perimarine environment. *Sediment. Geol.* 17, 1–234.
- Wilson, J., Savage, D., Bond, A., Watson, S., Pusch, R., Bennett, D., 2011. Bentonite: a Review of Key Properties, Processes and Issues for Consideration in the UK Context. Quintessa Report QRS-1378ZG-1.1 for the NDA-RWMD. Quintessa, Henley-on-Thames, UK.